First-principles study of hexagonal tungsten trioxide: Nature of lattice distortions and effect of potassium doping

Peter Krüger,* Issam Koutiri, and Sylvie Bourgeois
ICB, UMR 6303 CNRS - Université de Bourgogne, F-21078 Dijon, France
(Received 6 October 2012; published 5 December 2012)

A density functional theory study is reported on pure and potassium doped tungsten trioxide. The nature of lattice distortions in the hexagonal phase is analyzed and a new symmetry group is proposed. The structure and stability of cubic, monoclinic, and hexagonal phases is studied as a function of potassium doping and an approximate phase diagram is derived. K_xWO_3 undergoes a monoclinic to hexagonal phase transition at $x \sim 3\%$.

DOI: 10.1103/PhysRevB.86.224102 PACS number(s): 61.50.Ah, 61.66.Fn

I. INTRODUCTION

Tungsten trioxide (WO_3) is an interesting material for catalysis[1] and gas sensing.[2] Upon alkali-metal doping, WO_3 forms tungsten bronzes with promising optoelectronic properties such as electrochromism.[3] Pure WO_3 has a rich phase diagram and undergoes several structural transitions in the temperature range 0–1000 K. The crystal structure is close to the ReO_3 type (defect perovskite), with corner sharing, W-centered oxygen octahedra which form a simple cubic lattice. This ideal cubic structure (c-WO_3) does not exist. Instead, lattice distortions reduce the symmetry to tetragonal, orthorhombic, monoclinic, or triclinic depending on temperature. At room temperature, the monoclinic γ phase (m-WO_3) with space group $P2_1/n$ is stable.[4,5] Using specific synthesis routes, another phase, with hexagonal structure (h-WO_3) can also be stabilized at room temperature. The h-WO_3 phase was first synthesized by Gerand *et al.*[6] by dehydration of $WO_3 \cdot 1/3H_2O$. Disregarding distortions, the authors proposed a simplified atomic structure with $P6/mmm$ symmetry. Schlasche and Schöllhorn[7] and Oi *et al.*[8] synthesized h-WO_3 from ammonium-containing precursors and reported somewhat different lattice parameters than those of Gerand *et al.*[6] Oi *et al.*[8] found a strongly distorted structure with $P6_3/mcm$ space group. The atomic positions could, however, not be fully determined and two different and equally likely data sets were reported. To date, it is not clear whether the three reported models correspond to different crystal structures, possibly due to different residual impurities (H_2O or NH_3),[9] or whether the differences between models are due to uncertainties in the structural refinements.

From the theoretical side, most studies have concentrated on the cubic and monoclinic phases.[10–14] For the hexagonal phase, only the simplified high-symmetry ($P6/mmm$) structure[6] has been considered.[15–17] To the best of our knowledge, the precise atomic structure and the nature of the lattice distortions in h-WO_3 has never been studied by first-principles theory.

The metastable hexagonal phase can also be stabilized by growing WO_3 nanostructures on appropriate surfaces. Gillet *et al.*[18] reported the formation of h-WO_3 nanorods on a muscovite(0001) surface. The K^+ ions present at the muscovite surface are believed to play a crucial role in stabilizing the h-WO_3 phase,[19,20] because bulk $K_{0.26}WO_3$ has hexagonal structure. Hexagonal K_xWO_3 has been calculated from first principles for $x = 1/3$,[15,16] but no systematic study of the stability of K_xWO_3 as a function of doping level x has been performed so far.

Here we report a density functional theory study on the structure and energetics of pure and K-doped WO_3, in cubic, monoclinic, and hexagonal phases. For pure WO_3 in the hexagonal phase, we find that the lattice is substantially distorted in agreement with experiment.[6,8] The calculated atomic structure has common features with several conflicting models, thus providing a synthesis of the experimental data. It is shown that upon K doping, WO_3 undergoes a monoclinic to hexagonal structural transition at doping level $x \sim 3\%$ and an approximate room-temperature phase diagram of K_xWO_3 is proposed.

II. COMPUTATION

The calculations were carried out using the plane-wave projector augmented wave code VASP[21,22] in the framework of density functional theory (DFT) with the exchange-correlation functional GGA-PBE (generalized gradient approximation-Perdew-Burke-Ernzerhof). The energy cutoff was set to 400 eV. The Brillouin zone of m-WO_3 and h-WO_3 was sampled on a Γ-centered $5 \times 5 \times 5$ k-space grid. For some supercell calculations of K_xWO_3, correspondingly fewer points were used such that the grid spacing Δk is approximately the same. Structural optimizations were performed by relaxing all atomic positions at a fixed cell volume and then searching the total energy minimum as a function of cell volume. We have also carried out some test calculations using the local density approximation (LDA). We found very similar results as with GGA-PBE, apart from the well-known fact that the equilibrium volume is systematically smaller in LDA than in GGA.

III. RESULTS AND DISCUSSION

A. Cubic and monoclinic phases

For the idealized cubic phase we find an energy of -36.274 eV and an equilibrium lattice constant of 3.82 Å, in good agreement with previous DFT-GGA results.[14,16] The calculated energy of the monoclinic phase is slightly lower, -36.396 eV per WO_3 unit, which implies that the cubic phase is unstable under monoclinic lattice distortion, in agreement with experiment. In the following we shall indicate energies per WO_3 unit and relative to the monoclinic phase, so

$E(\text{m-WO}_3) = 0$ by definition and $E(\text{c-WO}_3) = 0.122$ eV. The calculated lattice parameters of m-WO_3 ($a = 7.63$, $b = 7.73$, $c = 7.75$ Å, and $\gamma = 90.5°$) agree well with most other theoretical values.[14,17] However, as usual for the GGA, they are slightly overestimated (1–4%) as compared to experiment ($a = 7.31$, $b = 7.54$, $c = 7.69$ Å, and $\gamma = 90.9°$).[4,5] The calculated atomic positions of m-WO_3 display qualitatively the same lattice distortions as in experiment. The amplitude of the distortions is, however, underestimated, especially for the oxygen sublattice. The O positions differ from the high-symmetry (c-WO_3) sites by up to 0.3 Å in experiment, but only up to 0.07 Å in the calculations. The agreement between experiment and theory is better for the W sites with a maximum displacement of 0.3 Å in experiment and 0.2 Å in theory. We conclude that the structure and energetics of the m-WO_3 phase can be qualitatively well reproduced with the present DFT-GGA scheme, even though the lattice parameters are slightly overestimated and the distortion of the O sublattice is underestimated.

B. Hexagonal phase

The atomic structure of h-WO_3 is not completely understood to date. Gerand *et al.*[6] suggested $P6_3/mcm$ as a likely space group. However, they determined the atomic positions only very approximately by assuming the higher symmetry group $P6/mmm$.

This simplified structure, denoted here H1, is depicted in Fig. 1 and summarized in Table I. In H1, the individual WO_6 octahedra have only a very weak tetragonal distortion. The W sites are located exactly at the centers and the O-O bonds have almost equal length (2.70 ± 0.04 Å).

In contrast, a h-WO_3 structure with considerably distorted octahedra was reported by Oi *et al.*[8] They proposed two equally likely models (denoted here as H2 and H3), with the same lattice constants and symmetry ($P6_3/mcm$) but different atomic positions, see Table I and Fig. 1(b). In H2, the O octahedron is strongly distorted in the (xy) plane, giving rise to two short O1-O1 bonds (2.3–2.4 Å). In H3, on the other hand, the O1 positions are the same as in H1. In both H2 and H3, the apical O2 sites are displaced in the (x,y) plane by 0.4–0.5 Å from the high-symmetry positions (0.5,0,0), which leads to some short O1-O2 bonds (2.4 Å). Moreover, the O2 sites are 12-fold with occupancy 0.5, that is, only 6 of the 12 equivalent sites are occupied [pink balls in Fig. 1(b)]. The W sites are displaced in the xy plane by 0.2 Å from the centers of the octahedra.

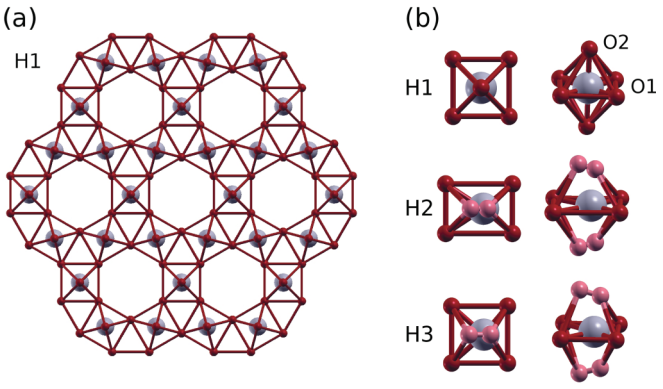

FIG. 1. (Color online) Experimental structures of hexagonal WO_3 (Refs. 6 and 8). W in gray and O in red and pink for occupancy 1 and 0.5, respectively. (a) Top view (along c axis) of model H1 (Ref. 6). (b) Top and side view of individual WO_6 octahedra in different models.

TABLE I. Structural models for hexagonal WO_3 from experimental Ref. 6 (H1) and Ref. 8 (H2, H3). Space group ("sym"), lattice constants (in Å), and atomic positions are given. For model H1 the cell origin and Wyckoff symbols have been adapted to the lower symmetry space group $P6_3/mcm$ for easy comparison with models H2 and H3. In H2 and H3 the occupancy of the 12k site (O2) is 50%.

Model	H1	H2	H3
sym	$P6/mmm$	$P6_3/mcm$	
a	7.298	7.324	7.324
c	7.798	7.663	7.663
c/a	1.069	1.046	1.046
W	6g (x,0,0.25)		
x	0.5	0.472	0.472
O1	12j (x,y,0.25)		
x	0.424	0.375	0.423
y	0.212	0.183	0.211
O2	6f (0.5,0,0)	12k (x,0,z)	
x	0.5	0.445	0.431
z	0.0	0.016	0.018

We have optimized the atomic structure of h-WO_3 in different symmetries, corresponding to the experimental models H1, H2, or H3, and without symmetry restriction. The results are summarized in Table II. For $P6/mmm$ symmetry, the calculated lattice constants agree within ±2% with the experimental values of model H1, but the calculated c/a ratio is 4% too small. The only internal structural parameter in this symmetry, x of O1, agrees within 1% with experiment.

TABLE II. Calculated structural data for hexagonal WO_3 in different symmetries. Energy in eV with respect to the monoclinic phase. See also legend of Table I.

Model	H1	H3	H4
sym	$P6/mmm$	$P6_3/mcm$	$P6_3cm$
a	7.463	7.509	7.456
c	7.672	7.583	7.764
c/a	1.028	1.010	1.041
W	6g (x,0,0.25)		6c (x,0,z)
x	0.5	0.467	0.474
z	0.25	0.25	0.228
O1	12j (x,y,0.25)		12d (x,y,z)
x	0.429	0.424	0.426
y	0.214	0.216	0.217
z	0.25	0.25	0.25
O2	6f (0.5,0,0)		6c (x,0,z)
x	0.5	0.5	0.497
z	0	0	−0.002
Energy	0.129	0.040	0.019

According to the experimental models H2 and H3[8] the six O2 atoms occupy 12 sites with occupancy 0.5. From a microscopic viewpoint, the question arises which six sites in the unit cell are actually occupied. In the calculation, a choice has to be made, and this necessarily breaks the $P6_3/mcm$ symmetry. The number of possibilities to choose 6 sites among 12 is huge (12!/6!/6!). Most of these possibilities can be discarded on physical grounds, because any two nearest neighbor O2 sites are only ∼1 Å apart and cannot be occupied at the same time (see the pairs of pink balls on the same side of the octahedra in Fig. 1.) This leaves $2^6 = 64$ physically acceptable configurations, many of which are equivalent by symmetry. We have tried several inequivalent configurations as initial conditions in the optimization. In all cases, the O2 atoms relaxed very near (<0.03 Å) the high symmetry position (0.5,0,0). This result automatically removes the problem of the right choice of the ($12k$) sites since (0.5,0,0) is a sixfold ($6f$) site in $P6_3/mcm$ symmetry. As for the O1 site, the optimized position agrees well with the H3 (and H1) model, see Table II. No solution was found corresponding to the strongly distorted O1 positions as given in model H2. We have carefully checked this by using H2 as initial structure of the optimization. Even then, the O1 atoms relaxed to the H3 positions. Thus the H2 model can be definitely ruled out. In all, two converged structures were obtained from the different initial configurations for the H2 and H3 models. The first one (denoted H3 in Table II) has $P6_3/mcm$ symmetry, as suggested by experiments.[6,8] It was obtained when the initial configuration had a mirror plane perpendicular to c. The W and O1 positions agree well with the experimental model H3. Significant discrepancy with the experimental data is found for the O2 positions (no distortion in calculation, as discussed before) and the c/a ratio, which is underestimated by 4%. The second converged structure (denoted H4, see Table II and Fig. 2) was obtained when the initial configuration had no symmetry at all. Nonetheless, the converged structure has, within a numerical error bar of ∼0.01 Å, space group symmetry $P6_3cm$. With respect to $P6_3/mcm$, one symmetry element is missing, namely the mirror plane perpendicular to c. Comparing the calculated structural parameters of H4 with the experimental values of H3, we see a slight (1–2%) overestimation of the lattice constants, as usual for GGA, but excellent agreement (∼0.5%) for the c/a ratio. Also the O1 and W coordinates agree very well, except that in H4, the W atoms are displaced from the center of the octahedron not only in the xy plane, as assumed in model H3, but also in the z direction, by about 0.2 Å, see Fig. 2. This extra distortion breaks the mirror plane perpendicular to **c** and thus lowers the symmetry from $P6_3/mcm$ to $P6_3cm$.

The displacement of W in the xy plane reduces the symmetry from $P6/mmm$ (model H1) to $P6_3/mcm$ (model H3) and lowers the energy very significantly by 0.09 eV (see Table II). The extra displacement of W along z in H4 lowers the energy further by 0.02 eV. The fact that the most stable structure H4 has $P6_3cm$ symmetry seems to disagree with experiment, where $P6_3/mcm$ was found as the most likely symmetry group. However, when taken alone, the W sublattice of H4 has exactly $P6_3/mcm$ symmetry and the positions of the W atoms agree almost perfectly (<0.5%) with the measured ones in H3.[8] To see this, the origin of the coordinate system of H4 in Table II can be shifted by $-0.022\mathbf{c}$. So in H4, the distortion of the hexagonal cell (c/a ratio) and the distorted W sublattice (taken alone) agree perfectly with the experiments of Oi *et al.*[8] These structural parameters have been determined most reliably since x-ray diffraction[8] and electron microscopy[6] measurements are very sensitive to the positions of the heavy element tungsten, but much less so to oxygen. The O positions could not be determined with certainty in the experiments. Instead, two equally likely models (H2 and H3) with quite different O sites were proposed from the same data.[8] In our lowest energy solution H4, the oxygen sublattice is hardly distorted and agrees well with the simple H1 model. The W atoms, however, show considerable distortion which was not fully accounted for in the experimental models H2 and H3, which disregarded the out-of-xy-plane displacement of the W atoms. The calculation reveals that the W atoms are displaced towards a face of the octahedron, rather than towards an edge as suggested in models H2 and H3. As a result, each W atom has three short W-O bonds (∼1.8 Å) and three long ones (2.0–2.1 Å), see Fig. 2(c). In the H4 structure, each O atom has one short and one long O-W bond, so from the oxygen perspective, the lattice distortion corresponds to a bond length asymmetry along the W-O-W lines, as in the monoclinic phase.[12] The H4 structure with $P6_3cm$ symmetry is probably the most regular realization of such an asymmetric W-O-W bonding in the h-WO_3 structure. The experimentally proposed $P6_3/mcm$ symmetry is not compatible with this W-O-W asymmetry in all three directions of the network, because in $P6_3/mcm$ the mirror plane perpendicular to **c** implies that the W-O bonds along **c** are of equal length.

Because the structural energy differences in Table II are quite small, we have checked the stability of the different phases by calculating the vibrational frequencies at the Γ point of the Brillouin zone. We found that in structures H1 and H3 (as well as in the cubic phase), there are several

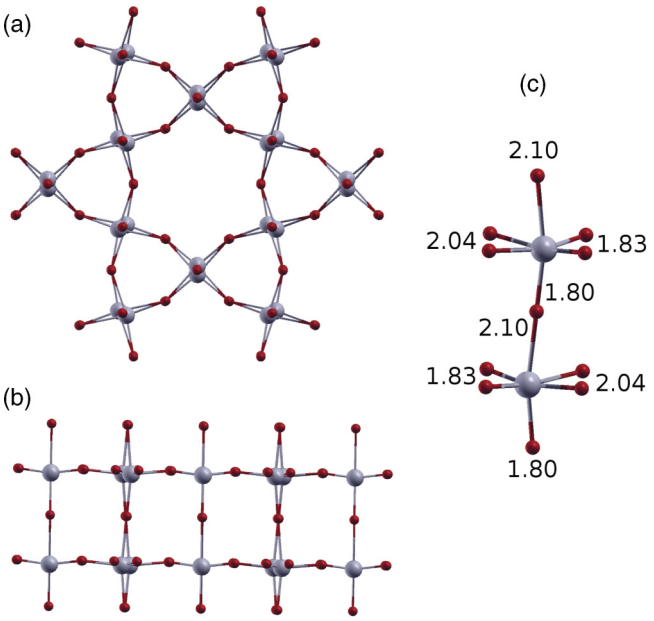

FIG. 2. (Color online) Calculated lowest energy structure H4 of hexagonal WO_3. (a) Top view (along c axis). (b) Side view. (c) Two WO_6 octahedra along c with bond lengths in Å.

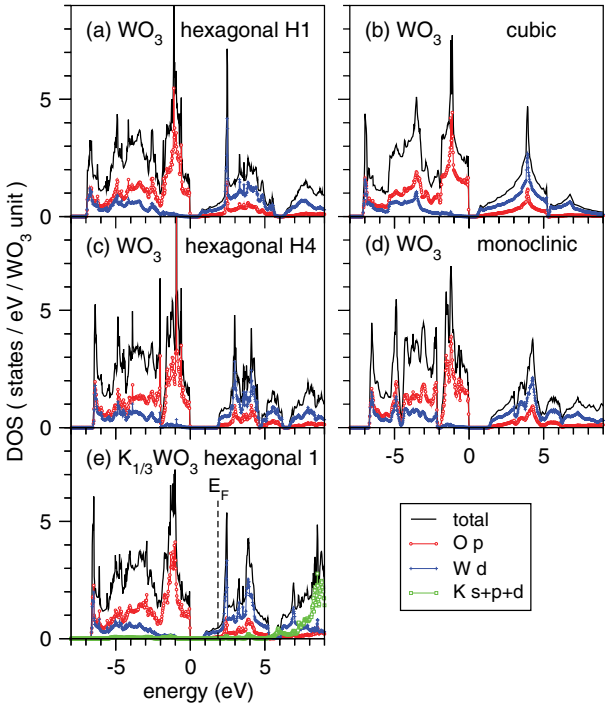

FIG. 3. (Color online) Density of states (DOS) of WO_3 in different phases (a)–(d) and of $K_{1/3}WO_3$ in hexagonal 1 phase (e). The local DOS were calculated with atomic radii of 0.75, 1.35, and 2.5 Å for O, W, and K, respectively. Energy is measured from the top of the valence band. The width of the insulating gap is (a) 0.51, (b) 0.48, (c) 1.83, and (d) 1.21 (in eV). The Fermi level lies in the band gap for (a)–(d) and is indicated as E_F in (e).

modes with imaginary frequencies of the order of 20 meV. This clearly shows that these structures are unstable with respect to lattice distortion in agreement with our total energy results. For the monoclinic and the H4 structure, in contrast, no modes with imaginary frequencies exist at the Γ point. For these two phases we have estimated the zero-point energy[23] in the Γ-point approximation. We found 0.279 eV for the monoclinic phase and 0.284 eV for H4, which indicates that the zero-point contribution is negligible for the relative structural energies.

C. Electronic structure

In Figs. 3(a)–3(d) the density of states (DOS) is plotted for the four studied structures of WO_3. The total DOS and the partial O-p and W-d DOS are shown. Other partial DOS (O-s,d and W-s, p) are negligible on this scale. The total DOS of the cubic and hexagonal H1 phase of WO_3 agree well with those obtained by Ingham *et al.*[16] The valence band is dominated by O-p and the conduction band by W-d states as an ionic bonding picture would suggest. However, except for the top of the valence band which is of almost pure O-p character, all bands are strongly hybridized between O-p and W-d states, which signals a strong covalency of the bonding. The DOS of cubic and hexagonal H1 phases are similar. The most obvious difference is the appearance in the hexagonal DOS of a sharp peak at 2.5 eV, which can be assigned to the existence of a very flat band in the whole Brillouin zone, as seen in Fig. 2 of Ref. 17. The DOS of the distorted phases (monoclinic and H4) is not very different from the corresponding undistorted ones (cubic and H1). Upon distortion, the bands become narrower and the DOS display more fine structure. For example, the dip at −2 eV develops into a tiny gap in the monoclinic phase. The most important effect of distortion is the increase of the insulating gap. When going from the cubic to the monoclinic phase the gap increases from 0.48 to 1.21 eV in agreement with other DFT-GGA calculations.[13,14,17] The calculated monoclinic gap is, however, much smaller than in experiment (∼3 eV[14]). This typical shortcoming of DFT may be corrected for by using many-body approaches such as the GW approximation or hybrid functionals.[14] Such approaches are, however, computationally much more demanding without improving the structural and energetic properties that we are mainly interested in here. In the hexagonal phase, too, the gap increases strongly upon distortion and the effect is even larger than in the cubic-monoclinic transition. The gap increases from 0.51 eV in the undistorted H1 structure to 1.83 eV in the distorted H4 structure.

D. K_xWO_3 phase diagram

Next we have studied the structure and energetics of potassium doped tungsten trioxide (K_xWO_3) as a function of x in the range $0 < x < 0.5$. The interstitial sites are known from the alkali bronzes. In the cubic phase the interstitial site is the center of the cube formed by eight W atoms. A K atom has thus 12 O nearest neighbors at a distance $a_c/\sqrt{2} \approx 2.7$ Å. The monoclinic cell corresponds to a $2 \times 2 \times 2$ cubic cell and has eight interstitial sites. In the hexagonal phase, the interstitial sites are located in the hexagonal "tunnels" formed by six connected WO_6 octahedra. A K atom has 12 O nearest neighbors at a distance of 3.3 Å. For the cubic and monoclinic phases, the calculations were performed in a $K_{8x}W_8O_{24}$ cell, which corresponds to the primitive cell of m-WO_3, and the $2 \times 2 \times 2$ supercell of c-WO_3. For the hexagonal phase, the primitive cell $K_{6x}W_6O_{18}$ was used. For one point, $x = 1/12 = 0.83$, bigger cells were needed, namely $K_2W_{24}O_{72}$ for the cubic and monoclinic, and $K_1W_{12}O_{36}$ for the hexagonal phase. In the calculations we have fixed the symmetry of the supercell to cubic, monoclinic, and hexagonal, respectively. The positions of all atoms and the cell volume have been fully optimized. In order to investigate the influence of lattice distortion in the hexagonal phase, we have considered two hexagonal systems, an "undistorted" one (h1) which contains a proper sixfold rotation axis and corresponds to the H1 structure in pure WO_3, and a distorted one (h2), which has only a threefold axis and corresponds to the H4 structure in pure WO_3.

Figure 4 shows the relative energies of K_xWO_3 in the different phases and the corresponding phase diagram. It is seen that the monoclinic phase is most stable only for very low K concentration. At a doping level of $x \sim 3\%$, the hexagonal phase becomes ground state until $x \sim 40\%$. For even higher K concentrations, the cubic phase is most stable.

The energy of the monoclinic phase falls on an almost straight line, which means that the insertion energy of a K atom is independent of the doping concentration (in the calculated range $0 < x < 0.5$). This indicates that K-K interaction is negligible which is also supported by our finding that for a given K concentration, the energy is independent (within 0.01 eV) of the choice of the occupied interstitial sites. In

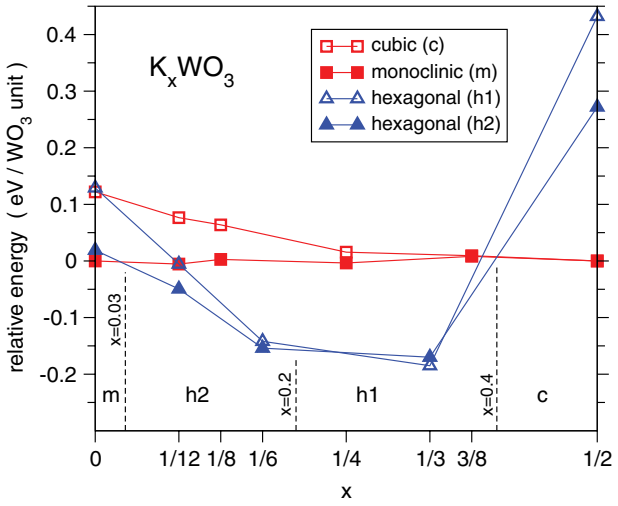

FIG. 4. (Color online) Stability of the different phases of K_xWO_3. Here the energy is measured relative to that of the monoclinic phase, linearly interpolated between $x = 0$ and $x = 0.5$. (This energy is $-36.396 - 3.27\,x$.) At the bottom, the corresponding, approximate phase diagram is shown with the stable phases and estimated phase boundaries.

contrast, the energy of the hexagonal K_xWO_3 is a highly nonlinear function of x. The energy of both h1 and h2 phases decreases quickly with x for $x < 1/6$, then much more slowly for $1/6 < x < 1/3$ before it rises sharply for $x > 1/3$. For $x > 1/12$, the curvature of $E(x)$ is clearly positive. This means that insertion of a K atom becomes energetically less and less favorable with increasing doping and indicates a repulsive K-K interaction. This may be seen as follows. The curvature d^2E/dx^2 times dx^2 directly gives the energy of the disproportioning reaction $2\ K_xWO_3 \rightarrow K_{x+dx}WO_3 + K_{x-dx}WO_3$. When $d^2E/dx^2 > 0$ this reaction is energetically not favored, so the system prefers a homogeneous distribution of K atoms, which means that the K atoms want to stay apart, that is, they interact repulsively. For the highly oxidized K^+ cations in K_xWO_3, strong K-K repulsion is of course expected from electrostatics. Our finding that the K-K interaction is negligible in monoclinic K_xWO_3 shows that the K^+-K^+ repulsion is efficiently screened by the negatively charged WO_3 matrix. In the hexagonal structure, the screening is much less efficient between K^+ ions in the same tunnel since the tunnels are large and the electrostatic potential along the tunnels is very flat.[15] For $x > 1/3$, strong K-K repulsion is also expected because nominally maximum doping (one K per interstitial site) is reached at $x = 1/3$. For $x = 1/2$, a tunnel segment of $c \sim 7.7$ Å is filled with three K atoms, such that the K-K distance becomes very short (2.6 Å).

It can be seen from Fig. 4 that the energy difference between the cubic and monoclinic phases decreases as a function of x and vanishes for $x > 0.35$. At the same time the atomic structure of the monoclinic phase approaches the cubic one: c/a goes to 1 and the W atoms move "back" to the center of the octahedra. The removal of the monoclinic lattice distortion through doping was already reported for electron-doped WO_3.[11] Qualitatively the same behavior is found for the hexagonal phase. The difference between the distorted structure h2 and the high-symmetry structure h1 fades away for $0 < x < 1/6$ and becomes negligible for $1/6 < x < 1/3$. In the overdoped, unstable regime $x > 1/3$, distortions develop again.

In Fig. 3(e) the DOS of $K_{1/3}WO_3$ is shown in its ground state hexagonal 1 structure. The valence and conduction bands are hardly changed from the corresponding undoped system [hexagonal H1, Fig. 3(a)] except that the states in the first 0.5 eV of the conduction band are filled and so the system becomes metallic. Qualitatively the same behavior was found for cubic alkali WO_3 bronzes.[16] In the whole valence band and the lower 5 eV of the conduction band of $K_{1/3}WO_3$, the orbital character is not changed from pure WO_3, and the local DOS on the K atoms [green curve in Fig. 3(e)] is negligible. Potassium orbitals contribute only to empty states at over 5 eV above the Fermi level. This analysis shows that the potassium atoms transfer their $4s$ electrons to the WO_3 matrix and K^+ forms purely ionic bonds with W and O.

IV. CONCLUSIONS

In summary, we have presented a first-principles study on pure and K-doped WO_3 in the relevant room temperature phases. The nature of the lattice distortions in hexagonal WO_3, which is an unsolved problem in the experimental literature, has been studied theoretically. The calculated ground state structure is in good agreement with experiment for the well-established part of the structure, namely lattice constants and W positions. We find that the W atoms are displaced from the center of the O_6 octahedra not only in the basal plane but also along c. This distortion corresponds to a bond length asymmetry along all W-O-W lines, and reduces the symmetry group from previously assumed $P6_3/mcm$ to $P6_3cm$. The structure and stability of K_xWO_3 has been studied for $x < 0.5$ and an approximate phase diagram has been established. It has been shown that upon K doping, monoclinic WO_3 becomes unstable with respect to the hexagonal phase when the doping concentration exceeds about 3%. Beyond the nominal maximum doping concentration ($x = 1/3$) of hexagonal K_xWO_3, the cubic phase becomes most stable.

ACKNOWLEDGMENTS

We are grateful for computing time provided by GENCI-CINES and the Centre de Ressources Informatiques of the Université de Bourgogne. We thank Dr. Stéphanie Bruyère for fruitful discussions.

*pkruger@u-bourgogne.fr

[1] D. G. Barton, M. Shtein, R. D. Wilson, S. L. Soled, and E. Iglesia, J. Phys. Chem. B **103**, 630 (1999).

[2] C. S. Rout, M. Hedge, and C. N. R. Rao, Sensors Actuators B: Chem. **128**, 488 (2008).

[3] C. G. Granqvist, Sol. Energy Mater. Sol. Cells **60**, 201 (2000).

[4] B. O. Loopstra and H. M. Rietveld, Acta Crystallogr. Sect. B **25**, 1420 (1969)

[5] P. M. Woodward, A. W. Sleight, and T. Vogt, J. Phys. Chem. Solids **56**, 1305 (1995).

[6]B. Gerand, G. Nowogrocki, J. Guenot, and M. Figlarz, J. Solid State Chem. **29**, 429 (1979).
[7]B. Schlasche and R. Schöllhorn, Rev. Chim. Miner. **19**, 534 (1982).
[8]J. Oi, A. Kishimoto, T. Kudo, and M. Hiratani, J. Solid State Chem. **96**, 13 (1992).
[9]I. M. Szilágyi, J. Madarász, G. Pokol, P. Király *et al.*, Chem. Mater. **20**, 4116 (2008).
[10]G. A. de Wijs, P. K. de Boer, R. A. de Groot, and G. Kresse, Phys. Rev. B **59**, 2684 (1999).
[11]A. D. Walkingshaw, N. A. Spaldin, and E. Artacho, Phys. Rev. B **70**, 165110 (2004).
[12]C. Lambert-Mauriat and V. Oison, J. Phys.: Condens. Matter **18**, 7361 (2006).
[13]M. N. Huda, Y. Yan, C.-Y. Moon, S.-H. Wei, and M. M. Al-Jassim, Phys. Rev. B **77**, 195102 (2008).
[14]F. Wang, C. Di Valentin, and G. Pacchioni, J. Phys. Chem. C **115**, 8345 (2011).
[15]F. Corà and C. R. A. Catlow, Phys. Status Solidi B **217**, 577 (2000).
[16]B. Ingham, S. C. Hendy, S. V. Chong, and J. L. Tallon, Phys. Rev. B **72**, 075109 (2005).
[17]D. B. Migas, V. L. Shaposhnikov, V. N. Rodin, and V. E. Borisenko, J. Appl. Phys. **108**, 093713 (2010).
[18]M. Gillet, K. Masek, V. Potin, S. Bruyère, B. Domenichini, S. Bourgeois, E. Gillet, and V. Matolin, J. Cryst. Growth **310**, 3318 (2008).
[19]S. Bruyère, V. Potin, M. Gillet, B. Domenichini, and S. Bourgeois, Thin Solid Films **517**, 6565 (2009).
[20]V. Potin, S. Bruyere, M. Gillet, B. Domechini, and S. Bourgeois, J. Phys. Chem. C **116**, 1921 (2012).
[21]G. Kresse and J. Furthmüller, Phys. Rev. B **54**, 11169 (1996).
[22]G. Kresse and D. Joubert, Phys. Rev. B **59**, 1758 (1999).
[23]R. A. Evarestov, E. Blokhin, D. Gryaznov, E. A. Kotomin, and J. Maier, Phys. Rev. B **83**, 134108 (2011).